ACS OMEGA

Open Access

http://pubs.acs.org/journal/acsodf

Article

An Integrated Analytical Approach for Screening Functional Post-Translational Modification Sites in Metabolic Enzymes

Xiaoxia Tan, Yue Han, Shengrui Zhai, Hanyang Dong, Tao Zhang,* and Kai Zhang*

Cite This: *ACS Omega* 2024, 9, 19003−19008

Read Online

ACCESS | Metrics & More | Article Recommendations | Supporting Information

ABSTRACT: Post-translational modifications (PTMs) are pivotal in the orchestration of diverse physiological and pathological processes. Despite this, the identification of functional PTM sites within the vast amount of data remains challenging. Conventionally, those PTM sites are discerned through labor-intensive and time-consuming experiments. Here, we developed an integrated analytical approach for the identification of functional PTM sites on metabolic enzymes via a screening process. Through gene ontology (GO) analysis, we identified 269 enzymes with lysine 2-hydroxyisobutyrylation (Khib) from our proteomics data set of *Escherichia coli*. The first round of screening was performed based on the enzyme structures/predicted structures using the TM-score engineer, a tool designed to evaluate the impact of PTM on the protein structure. Subsequently, we examined the influence of Khib on the enzyme−substrate interactions through both static and dynamic analyses, molecular docking, and molecular dynamics simulation. Ultimately, we identified NfsB K181hib and ThiF K83hib as potential functional sites. This work has established a novel analytical approach for the identification of functional protein PTM sites, thereby contributing to the understanding of Khib functions.

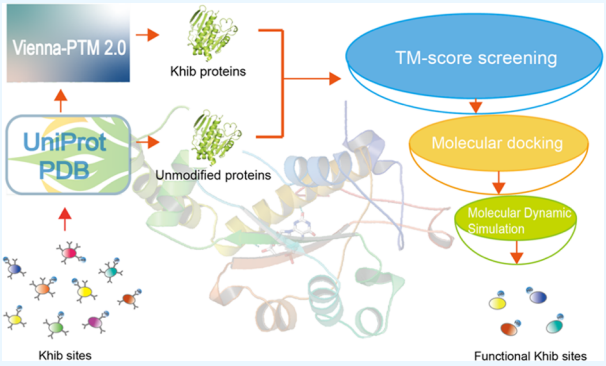

INTRODUCTION

Post-translational modifications (PTMs) are essential for the regulation of protein functions in various biological processes. While a vast amount of PTM data sets have been acquired, understanding these modifications is crucial for deciphering protein functions. For example, tyrosine phosphorylation is recognized to play an important role in cell signal transduction,[1−4] while ubiquitination is involved in inducing unstructured regions for proteasome interaction and regulation of protein degradation.[5,6] Despite the increasing discovery of new PTMs (e.g., acylation), the functional significance of many PTMs remains unclear, posing a significant challenge to fully understand their functional roles.

The advancement of mass spectrometry and enrichment techniques has led to a significant increase in the identification of lysine acylation, indicating its widespread biological implications. For instance, lysine lactylation (Kla) may be associated with dysregulated cancer metabolism.[7] Lysine crotonylation (Kcr) has been found in active promoters or potential enhancers in human somatic cells and mouse male germ cells.[8] And aberrant lysine succinylation (Ksucc) is strongly linked to human diseases such as cancer and neurodegenerative diseases.[9] However, the functional PTM sites are far from being completely understood, considering the high prevalence of lysine acylation. Therefore, it is crucial to develop a novel method for determining functional PTM sites from the extensive database.

Wet experiments are the primary approach for discovering functional PTM sites, which are typically costly and time-consuming. With the rapid development of bioinformatics, the field of protein structure prediction has advanced significantly. Currently, computational tools can predict the potential function of PTMs,[10] such as phosphorylation, ubiquitination, and acetylation, by using large amounts of biological data. However, due to insufficient knowledge, identifying the functional sites of newly discovered PTMs remains difficult.

Here, we developed a novel approach to screen functional PTM sites (Figure 1). First, we categorized the metabolic enzymes with lysine 2-hydroxyisobutyrylation (Khib) from our previous proteomics data set of *Escherichia coli*. Subsequently, we conducted screening using TM-score, followed by molecular docking and molecular dynamics (MD) simulation to determine functional Khib sites. Ultimately, we identified NfsB K181hib and ThiF K83hib as potential functional sites. Our approach offers a promising method for predicting and

Received: November 29, 2023
Revised: April 7, 2024
Accepted: April 10, 2024
Published: April 18, 2024

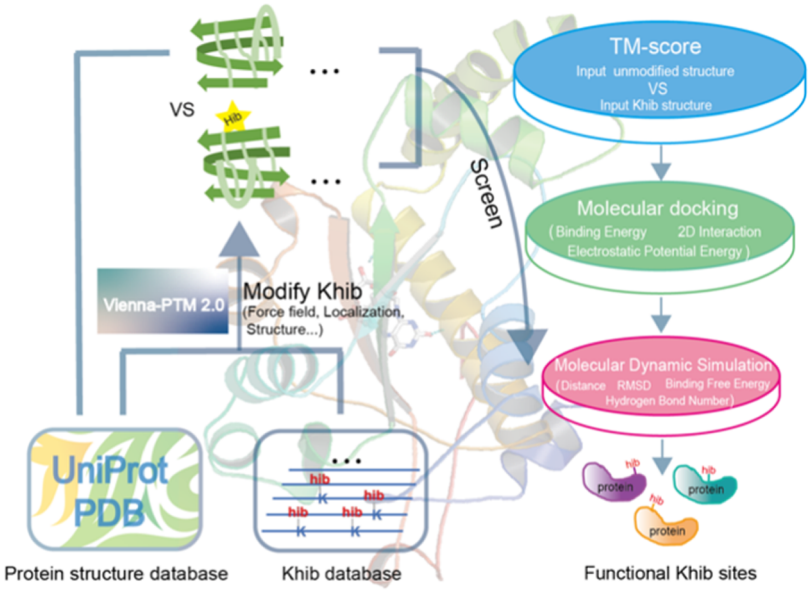

Figure 1. Flowchart for the screening of functional Khib sites by an integrated analytical approach (TM-score, molecular docking, and dynamics simulation) in *E. coli*.

screening functional PTM sites, thereby contributing to the comprehensive understanding of PTMs in cellular regulation.

EXPERIMENTAL DESCRIPTION

A total of 1137 proteins containing 7122 specific Khib sites were screened to identify the functional Khib sites. First, the structures of proteins with and without Khib sites were compared using the TM-score website to initially evaluate the impact of the Khib site. Subsequently, the proteins displaying obvious structural changes underwent molecular docking to further analyze the effect of the Khib site on substrate binding. The protein structures with unmodified and several different Khib sites, respectively, docked with the same substrate to compare the binding strength. A genetic algorithm was used to search for the optimal binding mode, and an empirical energy function was employed to estimate the binding energy. The docking box size was set to 40 × 40 × 40 Å, and the other docking parameters were kept at their default values. Based on the comparison of docking energy, proteins with a significant energy difference between the unmodified and Khib sites were selected for MD simulation. The optimal docking model of the substrate within the protein was considered the initial structure and placed in a cubic box with the SPC water model. To neutralize the system, chloride or sodium ions were randomly added to the simulation box. The energy minimization of the entire system was conducted over 50,000 steps using the steepest descent method. After minimization, a 500 ps NVT equilibration at 300 K and a 500 ps NPT equilibration at 1 bar were performed. The conventional molecular dynamics (MD) simulation was run for 100 ns with a time interval of 2 fs. During the MD simulations, the long-range Coulombic interactions were handled by using the particle mesh Ewald (PME) method. The trajectory of MD was utilized to calculate the root-mean-square deviation (RMSD), distance, number of hydrogen bonds, and binding free energy.

RESULTS AND DISCUSSION

The Characterization of Khib Omics in *E. coli*. Khib was originally discovered on histones in eukaryotic cells.[11] Soon afterward, we reported that Khib is a kind of conserved PTM and widely existed in prokaryotes,[12] further demonstrating that CobB is an extensive lysine de-2-hyroxyisobutyryltransferase, which mediates Khib of metabolic enzyme to regulate glycolysis in prokaryotes,[13] and that TmcA is a lysine 2-hydroxyisobutyryltransferase, which regulates transcription through a Khib-mediated molecular mechanism.[14] We revealed the regulation mechanism of Khib in prokaryote; however, the functional Khib sites we have known are still very limited.

Here, we first analyzed the characterization of the Khib sites that were collected from our previous study. A total of 7122 Khib sites were identified on 1137 proteins in *E. coli* (Table S1). The amount of Khib sites on each protein was counted (Figure S1A,B), and 240 proteins with over 10 Khib sites were found. To understand the significance of Khib sites in prokaryotes, we performed GO enrichment analysis of the 1137 substrate proteins of Khib. We further found that Khib proteins are enriched in metabolism and biosynthesis and occur mainly in mitochondrion, ribosomes, and cytosols with diverse binding activities (Figure S1C), suggesting that Khib may have an important effect on metabolism. Given that metabolic enzymes are the core basis of generating materials and energy in cell activities, we focused on the effect of Khib on the activities of 269 metabolic enzymes.

Screening by TM-Score. It has been known that the basic function of metabolic enzyme is to catalyze the transformation of metabolites, requiring that the metabolites (ligands) bind with metabolic enzymes. We screened protein structures based on the following conditions: (1) we prefer to choose the protein structures analyzed by X-ray, which are more reliable; (2) the protein structure analyzed by X-ray should contain Khib sites and the highest resolution. We reasonably hypothesized that the key Khib sites may have an effect on the structures of metabolic enzymes. Thus, we collected the protein structures of metabolic enzymes with Khib and corresponding ligand structures.

To examine preliminarily the influence of Khib on substrates, we chose TM-score, which is a metric for assessing the topological similarity of protein structures to native

https://doi.org/10.1021/acsomega.3c09514
ACS Omega 2024, 9, 19003−19008

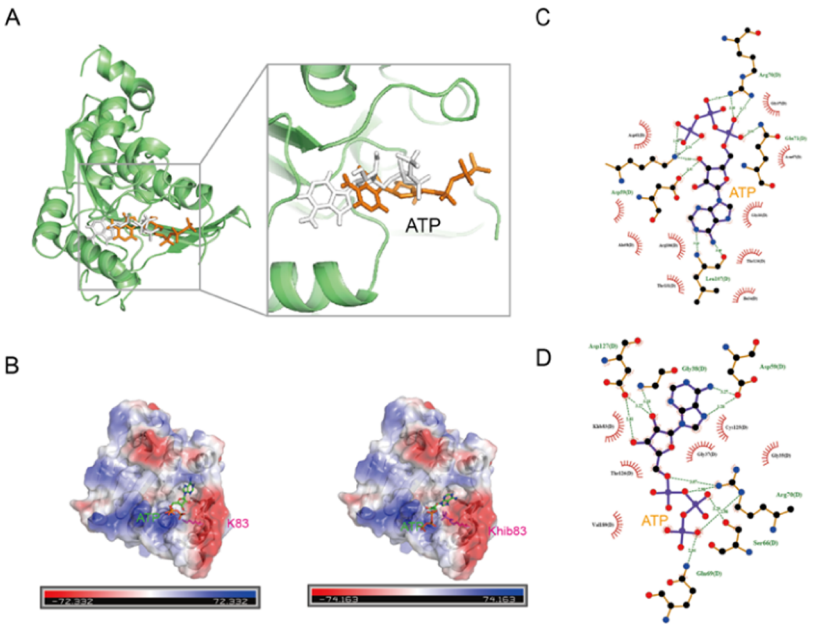

Figure 2. Molecular docking results of ThiF. (A) Three-dimensional (3D) analysis of ThiF-ATP and ThiF K83hib-ATP systems, molecular docking result. (B) Electrostatic potential surface of ThiF-ATP and ThiF K83hib-ATP systems, molecular docking result. (C) Hydrogen bonds and hydrophobic interactions between ThiF and ATP as shown by LigPlot+, setting the docking box at 40 × 40 × 40 Å. (D) Hydrogen bonds and hydrophobic interactions between ThiF K83hib and ATP as shown by LigPlot+, setting the docking box at 40 × 40 × 40 Å.

structures using the TM-Score program.[15] The quality of the protein prediction model was assessed by referring to several metrics.[16] For the proteins with both experimentally determined structure and ligand binding information, the TM-score value was calculated through the TM-Score program after the addition of the Vienna-PTM 2.0 modification, a resource for exploring PTMs using MD simulations.[17−19] By executing 1363 calculations based on TM-score engineer, 122 Khib sites (about 10%) were screened out as candidates (Table S2 and Figure S2).

Assessment by Molecular Docking. To further determine whether Khib influences the activity of the candidate proteins, we conduct static analysis by calculating their interactions with substrates using molecular docking. To compare the effect of PTM effectively on the substrate, we divided the receptor into two different states, unmodified and modified (Khib), which are bound to the same substrate. That is, two sets of different systems were constructed for the control experiments. Thus, 122 Khib sites were docked with their substrates, and as shown in Table S3 and Figure S3, NfsB K181hib, ThiF K83hib, MtnN K47hib, and YdhF K83hib show the obvious differences in binding energy between the Khib group and the correspondingly unmodified group.

The two-dimensional (2D) interactions of proteins NfsB, ThiF, MtnN, and YdhF with their ligands were further analyzed using LigPlot+ software, the electrostatic potential energy was calculated using PyMOL software, and the optimal binding conformation of the ligand was also displayed. The binding positions of FMN within NfsB-FMN and NfsB K181hib-FMN differ by a tiny offset distance (1.0 Å) after the two complexes, NfsB-FMN and NfsB K181hib-FMN, are superimposed. This is also the case with YdhF-NAP and YdhF K83hib-NAP (3.9 Å) (Figure S5A). However, the positions of the small molecules in the other two control groups, ThiF-ATP and ThiF K83hib-ATP (8.7 Å; Figure 2A), and MtnN-DF9 and MtnN K47hib-DF9 (6.9 Å; Figure S4A), have shifted significantly after docking. By comparing the overall electrostatic potential energy of the two systems, we found that there is an obvious difference between the two docking systems NfsB-FMN and NfsB K181hib-FMN (1.683 kcal/mol; Figure S6B), as well as ThiF-ATP and ThiF K83hib-ATP (1.831 kcal/mol) (Figure 2B). The difference between MtnN-DF9 and MtnN K47hib-DF9 (1.145 kcal/mol) (Figure S4B) and YdhF-NAP and YdhF K83hib-NAP (0.133 kcal/mol) (Figure S5B) are both not significant. Each system's hydrophobic and hydrogen bond interactions differ in the 2D interaction study. After docking with NfsB-FMN, the hydrogen bonding of the NfsB K181hib-FMN system varies significantly (Figure S6C,D). The remaining three control groups, YdhF-NAP and YdhF K83hib-NAP (Figure S5C,D), MtnN-DF9 and MtnN K47hib-DF9 (Figure S4C,D), and ThiF K83hib-ATP and ThiF-ATP (Figure 2C,D), were primarily represented by the hydrophobic interaction difference. In summary, the docking results suggested that four Khib sites have an obvious effect on the protein function from a static perspective, and then MD simulation was applied to examine the specific effects from a dynamic perspective.

Analysis by Molecular Dynamics Simulations. In MD simulations (100 ns), the effect of Khib on the structure (the initial structure is the original structure downloaded from the PDB) was further analyzed in detail after molecular docking. For this purpose, we conducted analysis from four aspects including the root-mean-square deviation (RMSD), hydrogen bond number, distances, and binding free energy. To observe the dynamic stability of the eight system complexes including NfsB-FMN and NfsB K181hib-FMN, ThiF-ATP and ThiF K83hib-ATP, MtnN-DF9 and MtnN K47hib-DF9, and YdhF-NAP and YdhF K83hib-NAP, we calculated RMSD using the starting structure. And thus, we found that the RMSD of the eight system complexes fluctuated slightly (Figures 3A, S7A,B, and S8A), indicating that all eight systems were stable.

https://doi.org/10.1021/acsomega.3c09514
ACS Omega 2024, 9, 19003−19008

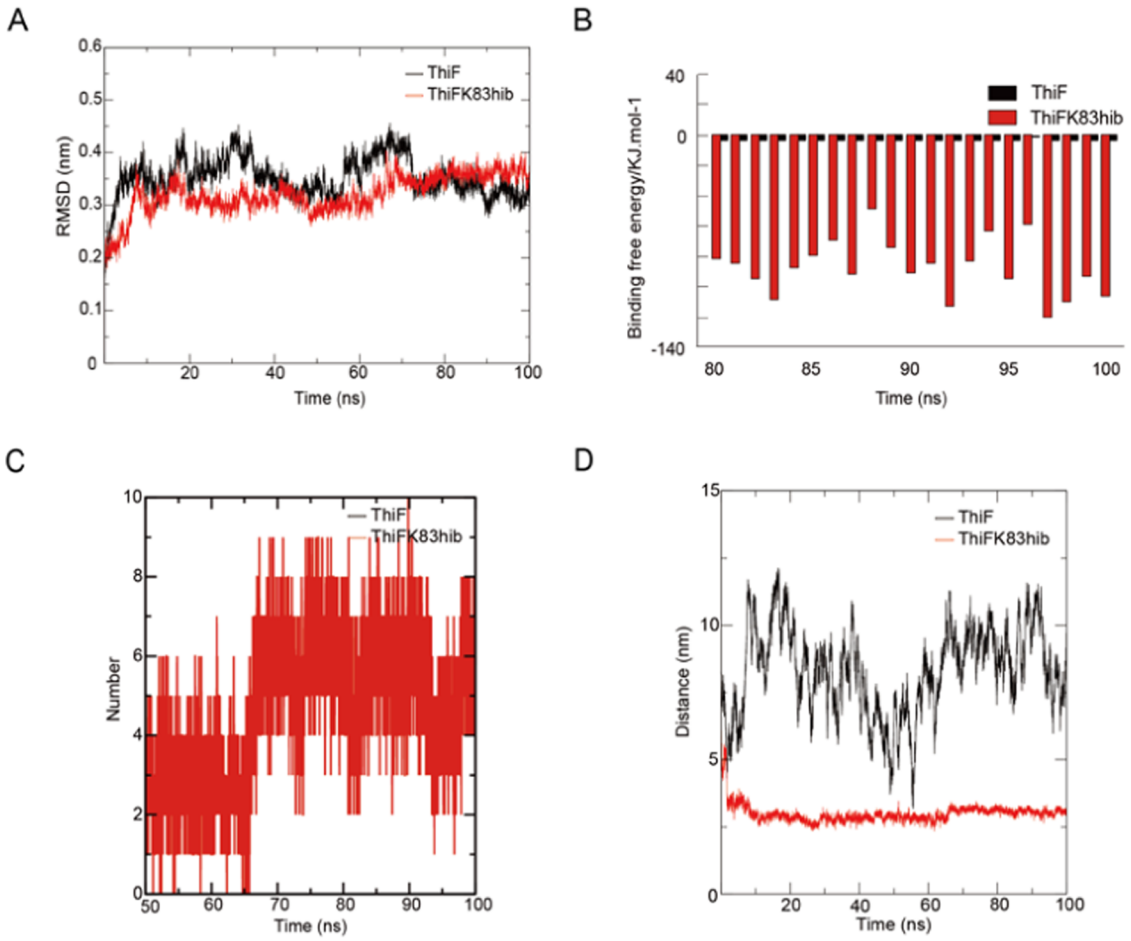

Figure 3. Molecular dynamics results of ThiF. (A) RMSD of the MD simulation for ThiF-ATP (black) and ThiF K83hib-ATP (red). (B) The binding free energy of the MD simulation for ThiF-ATP (black) and ThiF K83hib-ATP (red). (C) The number of hydrogen bonds of the MD simulation from 50 to 100 ns for ThiF-ATP (black) and ThiF K83hib-ATP (red). (D) The distance of the MD simulation for ThiF-ATP (black) and ThiF K83hib-ATP (red). The distance indicates the distance between the ThiF K83 side-chain nitrogen atom and the ATP central carbon atom.

Given that the hydrogen bond number contributes to the stability of the system, we further calculated the number of hydrogen bonds in the last 50 ns simulation of the eight systems. The geometric criteria for hydrogen bond formation between the ligand and acceptor are kept within 3.5 Å, and the angle between the donor and acceptor is set at 30 Å. Next, we measured the distance between the nitrogen atom on the side chain of the modification site and the central carbon atom of the ligand in the eight systems, given that such distances can better reflect the effect on binding. Furthermore, binding free energy can be effectively used to evaluate the affinity trend between the protein and ligand, and a more negative value indicates a more stable binding between the protein and ligand, whereas we finally computed the binding energy based on the conformations extracted from the last 50 ns simulation trajectories. In the results of the aforesaid analysis, there are obvious differences between NfsB-FMN and NfsB K181hib-FMN and ThiF-ATP and ThiF K83hib-ATP, compared to other systems (Figure S7C−F).

Next, we found that the number of hydrogen bonds varies greatly in the NfsB-FMN and NfsB K181hib-FMN systems (Figure S8C). During the simulation, NfsB-FMN can establish stable hydrogen bond connections. Furthermore, we discovered that the two systems' distance fluctuations were varied (Figure S8D). The average binding energies of NfsB-FMN and NfsB K181hib-FMN were −80.480 and −23.871 kJ/mol (Figure S8B), respectively. The NfsB-FMN systems have lower binding free-energy values, which indicates that the binding affinity is stronger. In two simulations of NfsB-FMN and NfsB K181hib-FMN, respectively, we retrieved the stable final structure (100 ns) to analyze the polarity action and electrostatic potential energy analysis in order to detect the microstructure changes. We found that there are two distinct systems (Figure S8G,H) containing residues that generate polarity when combined with FMN. The electrostatic potential energy distributions of NfsB-FMN and NfsB K181hib-FMN systems have obvious differences (Figure S8E,F). Thus, these results suggest that K181hib blocks the binding between FMN and NfsB and reduces the activity of NfsB.

The creation of hydrogen bonds in the ThiF K83hib-ATP system increased, reaching a maximum of 10 hydrogen links, while no hydrogen bonds formed in the ThiF-ATP system (Figure 3C). As a result, ThiF K83hib-ATP can establish stable hydrogen-bonding connections during the simulation. In the distance, K83 and ATP are particularly distinguished from K83hib and ATP (Figure 3D). Moreover, ThiF-ATP and ThiF K83hib-ATP had average binding energies of −3.637 and −87.704 kJ/mol, respectively (Figure 3B). Lower binding free-energy values for the ThiF K83hib-ATP systems imply a higher binding affinity. These results showed that K83hib may

https://doi.org/10.1021/acsomega.3c09514
ACS Omega 2024, 9, 19003−19008

promote the binding between ATP and ThiF. Notably, the effect of ThiF K83hib on the protein structure and function had been verified by the previous study.[20]

CONCLUSIONS

In summary, we developed an integrated analytical approach for screening functional PTM sites in metabolic enzymes. By the use of Khib on metabolism enzymes as a paradigm, we showed a multistep screening method (TM-score, molecular docking, and MD simulation) and identified NfsB K181hib and ThiF K83hib as functional Khib sites in *E. coli*. This study develops a new method for the screening and predicting functional sites of new protein modifications, providing a basis for the function and physiological consequence study of Khib.

ASSOCIATED CONTENT

Supporting Information

The Supporting Information is available free of charge at https://pubs.acs.org/doi/10.1021/acsomega.3c09514.

Experimental details, supporting figures (Figures S1−S8), and supporting tables (Tables S2 and S3) (PDF)

Protein and ligand structures and related parameter files used in MD simulations (Table S1) (XLSX)

AUTHOR INFORMATION

Corresponding Authors

Tao Zhang − *School of Biomedical Engineering, Tianjin Medical University, Tianjin 300070, China*; Email: zhangtao@tmu.edu.cn

Kai Zhang − *The Province and Ministry Co-Sponsored Collaborative Innovation Center for Medical Epigenetics, Key Laboratory of Immune Microenvironment and Disease (Ministry of Education), Tianjin Key Laboratory of Medical Epigenetics, Department of Biochemistry and Molecular Biology, School of Basic Medical Sciences, Tianjin Medical University, Tianjin 300070, China*; orcid.org/0000-0003-2800-0531; Email: kzhang@tmu.edu.cn

Authors

Xiaoxia Tan − *The Province and Ministry Co-Sponsored Collaborative Innovation Center for Medical Epigenetics, Key Laboratory of Immune Microenvironment and Disease (Ministry of Education), Tianjin Key Laboratory of Medical Epigenetics, Department of Biochemistry and Molecular Biology, School of Basic Medical Sciences, Tianjin Medical University, Tianjin 300070, China*

Yue Han − *The Province and Ministry Co-Sponsored Collaborative Innovation Center for Medical Epigenetics, Key Laboratory of Immune Microenvironment and Disease (Ministry of Education), Tianjin Key Laboratory of Medical Epigenetics, Department of Biochemistry and Molecular Biology, School of Basic Medical Sciences, Tianjin Medical University, Tianjin 300070, China*

Shengrui Zhai − *The Province and Ministry Co-Sponsored Collaborative Innovation Center for Medical Epigenetics, Key Laboratory of Immune Microenvironment and Disease (Ministry of Education), Tianjin Key Laboratory of Medical Epigenetics, Department of Biochemistry and Molecular Biology, School of Basic Medical Sciences, Tianjin Medical University, Tianjin 300070, China*

Hanyang Dong − *The Province and Ministry Co-Sponsored Collaborative Innovation Center for Medical Epigenetics, Key Laboratory of Immune Microenvironment and Disease (Ministry of Education), Tianjin Key Laboratory of Medical Epigenetics, Department of Biochemistry and Molecular Biology, School of Basic Medical Sciences, Tianjin Medical University, Tianjin 300070, China*

Complete contact information is available at: https://pubs.acs.org/10.1021/acsomega.3c09514

Author Contributions

The manuscript was written through contributions of all authors. All authors have given approval to the final version of the manuscript.

Notes

The authors declare no competing financial interest.
Any additional relevant notes should be placed here.

ACKNOWLEDGMENTS

This work was supported by the National Natural Science Foundation of China (Nos. 22074103, 22274114, 32101023, and 21874100), the Natural Science Foundation of Guangdong Province (No. 2022A1515011810), the China Postdoctoral Science Foundation (No. 2021M702067), and the Talent Excellence Program from Tianjin Medical University.

REFERENCES

(1) Mateus, A.; Kurzawa, N.; Becher, I.; Sridharan, S.; Helm, D.; Stein, F.; Typas, A.; Savitski, M. M. Thermal Proteome Profiling for Interrogating Protein Interactions. *Mol. Syst. Biol.* **2020**, *16* (3), No. e9232.

(2) Potel, C. M.; Kurzawa, N.; Becher, I.; Typas, A.; Mateus, A.; Savitski, M. M. Impact of Phosphorylation on Thermal Stability of Proteins. *Nat. Methods* **2021**, *18* (7), 757−759.

(3) Needham, E. J.; Hingst, J. R.; Parker, B. L.; Morrison, K. R.; Yang, G.; Onslev, J.; Kristensen, J. M.; Højlund, K.; Ling, N. X. Y.; Oakhill, J. S.; Richter, E. A.; Kiens, B.; Petersen, J.; Pehmøller, C.; James, D. E.; Wojtaszewski, J. F. P.; Humphrey, S. J. Personalized Phosphoproteomics Identifies Functional Signaling. *Nat. Biotechnol.* **2022**, *40* (4), 576−584.

(4) Cantley, L. C. The Phosphoinositide 3-Kinase Pathway. *Science* **2002**, *296* (5573), 1655−1657.

(5) Carroll, E. C.; Greene, E. R.; Martin, A.; Marqusee, S. Site-Specific Ubiquitination Affects Protein Energetics and Proteasomal Degradation. *Nat. Chem. Biol.* **2020**, *16* (8), 866−875.

(6) Yang, X.; Wang, Z.; Li, X.; Liu, B.; Liu, M.; Liu, L.; Chen, S.; Ren, M.; Wang, Y.; Yu, M.; Wang, B.; Zou, J.; Zhu, W.-G.; Yin, Y.; Gu, W.; Luo, J. SHMT2 Desuccinylation by SIRT5 Drives Cancer Cell Proliferation. *Cancer Res.* **2018**, *78* (2), 372−386.

(7) Zhang, D.; Tang, Z.; Huang, H.; Zhou, G.; Cui, C.; Weng, Y.; Liu, W.; Kim, S.; Lee, S.; Perez-Neut, M.; Ding, J.; Czyz, D.; Hu, R.; Ye, Z.; He, M.; Zheng, Y. G.; Shuman, H. A.; Dai, L.; Ren, B.; Roeder, R. G.; Becker, L.; Zhao, Y. Metabolic Regulation of Gene Expression by Histone Lactylation. *Nature* **2019**, *574* (7779), 575−580.

(8) Tan, M.; Luo, H.; Lee, S.; Jin, F.; Yang, J. S.; Montellier, E.; Buchou, T.; Cheng, Z.; Rousseaux, S.; Rajagopal, N.; Lu, Z.; Ye, Z.; Zhu, Q.; Wysocka, J.; Ye, Y.; Khochbin, S.; Ren, B.; Zhao, Y. Identification of 67 Histone Marks and Histone Lysine Crotonylation as a New Type of Histone Modification. *Cell* **2011**, *146* (6), 1016−1028.

(9) Alleyn, M.; Breitzig, M.; Lockey, R.; Kolliputi, N. The Dawn of Succinylation: A Posttranslational Modification. *Am. J. Physiol.: Cell Physiol.* **2018**, *314* (2), C228−C232.

(10) Tunyasuvunakool, K.; Adler, J.; Wu, Z.; Green, T.; Zielinski, M.; Žídek, A.; Bridgland, A.; Cowie, A.; Meyer, C.; Laydon, A.; Velankar, S.; Kleywegt, G. J.; Bateman, A.; Evans, R.; Pritzel, A.; Figurnov, M.; Ronneberger, O.; Bates, R.; Kohl, S. A. A.; Potapenko, A.; Ballard, A. J.; Romera-Paredes, B.; Nikolov, S.; Jain, R.; Clancy, E.;

Reiman, D.; Petersen, S.; Senior, A. W.; Kavukcuoglu, K.; Birney, E.; Kohli, P.; Jumper, J.; Hassabis, D. Highly Accurate Protein Structure Prediction for the Human Proteome. *Nature* **2021**, *596* (7873), 590−596.
(11) Dai, L.; Peng, C.; Montellier, E.; Lu, Z.; Chen, Y.; Ishii, H.; Debernardi, A.; Buchou, T.; Rousseaux, S.; Jin, F.; Sabari, B. R.; Deng, Z.; Allis, C. D.; Ren, B.; Khochbin, S.; Zhao, Y. Lysine 2-Hydroxyisobutyrylation Is a Widely Distributed Active Histone Mark. *Nat. Chem. Biol.* **2014**, *10* (5), 365−370.
(12) Dong, H.; Guo, Z.; Feng, W.; Zhang, T.; Zhai, G.; Palusiak, A.; Rozalski, A.; Tian, S.; Bai, X.; Shen, L.; Chen, P.; Wang, Q.; Fan, E.; Cheng, Z.; Zhang, K. Systematic Identification of Lysine 2-Hydroxyisobutyrylated Proteins in Proteus Mirabilis. *Mol. Cell Proteomics* **2018**, *17* (3), 482−494.
(13) Dong, H.; Zhai, G.; Chen, C.; Bai, X.; Tian, S.; Hu, D.; Fan, E.; Zhang, K. Protein Lysine De-2-Hydroxyisobutyrylation by CobB in Prokaryotes. *Sci. Adv.* **2019**, *5* (7), No. eaaw6703.
(14) Dong, H.; Zhao, Y.; Bi, C.; Han, Y.; Zhang, J.; Bai, X.; Zhai, G.; Zhang, H.; Tian, S.; Hu, D.; Xu, L.; Zhang, K. TmcA Functions as a Lysine 2-Hydroxyisobutyryltransferase to Regulate Transcription. *Nat. Chem. Biol.* **2022**, *18* (2), 142−151.
(15) Zhang, Y.; Skolnick, J. Scoring Function for Automated Assessment of Protein Structure Template Quality. *Proteins* **2004**, *57* (4), 702−710.
(16) Turzo, S. B. A.; Seffernick, J. T.; Rolland, A. D.; Donor, M. T.; Heinze, S.; Prell, J. S.; Wysocki, V. H.; Lindert, S. Protein Shape Sampled by Ion Mobility Mass Spectrometry Consistently Improves Protein Structure Prediction. *Nat. Commun.* **2022**, *13*, No. 4377.
(17) Margreitter, C.; Petrov, D.; Zagrovic, B. Vienna-PTM Web Server: A Toolkit for MD Simulations of Protein Post-Translational Modifications. *Nucleic Acids Res.* **2013**, *41*, W422−W426.
(18) Petrov, D.; Margreitter, C.; Grandits, M.; Oostenbrink, C.; Zagrovic, B. A Systematic Framework for Molecular Dynamics Simulations of Protein Post-Translational Modifications. *PLoS Comput. Biol.* **2013**, *9* (7), No. e1003154.
(19) Margreitter, C.; Reif, M. M.; Oostenbrink, C. Update on Phosphate and Charged Post-Translationally Modified Amino Acid Parameters in the GROMOS Force Field. *J. Comput. Chem.* **2017**, *38* (10), 714−720.
(20) Xu, X.; Wang, T.; Niu, Y.; Liang, K.; Yang, Y. The Ubiquitin-like Modification by ThiS and ThiF in *Escherichia coli*. *Int. J. Biol. Macromol.* **2019**, *141*, 351−357.

https://doi.org/10.1021/acsomega.3c09514
ACS Omega 2024, 9, 19003−19008